

# Influence of Camera's Optical Axis Non-perpendicularity on Measurement Accuracy of Two-dimensional Digital Image Correlation

A. Hijazi <sup>a,\*</sup>, A. Friedl <sup>b</sup> and C. J. Kähler <sup>b</sup>

<sup>a</sup> Department of Mechanical Engineering, The Hashemite University, Zarka, Jordan.

<sup>b</sup> Institute of Fluid Mechanics and Aerodynamics, Universität der Bundeswehr München, Neubiberg, Germany.

## Abstract

The two-dimensional digital image correlation technique is very commonly used in a wide variety of solid mechanics applications for measuring in-plane deformations of plannar surfaces. The perpendicularity of the camera's optical axis to the surface being observed is one of the basic conditions for the validity of the measurement. Small magnitudes of camera misalignment angles, up to two or three degrees, can go easily unnoticed during the initial setting of the experimental setup especially when the stand-off-distance between the camera and the surface is not small. In the work presented in this paper we investigate the errors in strain measurements caused by the non-perpendicularity of the camera's optical axis, with respect to the surface being observed, both theoretically and experimentally. In-plane rigid-body-translations in the directions perpendicular and parallel to the camera tilt axis are used for estimating the resulting strain errors. Results show that the non-perpendicularity of the camera causes errors in both the normal and shear strains. Misalignment angles as small as 2° are found to cause strain error greater than 10<sup>3</sup> μ-strains. The magnitude of strain error is found to increase linearly with both the misalignment angle and the magnitude of in-plane translation while it is inversely related to the stand-off-distance. The analyses show that simple in-plane rigid-body-translations experiments can be used to estimate the resulting strain errors and more importantly to detect and hence correct any existing non-perpendicularity between the camera's optical axis and the target surface. Experiments show that misalignment angles smaller than 1° can be detected using in-plane rigid-body-translations.

© 2011 Jordan Journal of Mechanical and Industrial Engineering. All rights reserved

Keywords: Digital image correlation, strain error, error analysis, camera non-perpendicularity, camera misalignment, in-plane translation.

## 1. Introduction

Nowadays, digital image correlation (DIC), also referred to as the digital speckle correlation method (DSCM), has become one of the most widely used full-field optical methods for motion and deformation measurements. The DIC method was first introduced by Sutton et al. [1] in the early 1980s and during the past three decades it underwent continuous modifications and significant improvements [2, 3]. In its simpler version, using a single camera, DIC is used for two-dimensional in-plane measurements (2D-DIC). Also, photogrammetric three-dimensional measurements (3D-DIC) [4] can be made using two cameras in stereo configuration. Besides the good measurement accuracy of the DIC method, it also offers other attractive features which include; relatively simple experimental setup, simple or no specimen preparation and low requirements for the measurement environment. All of that have made the DIC method extremely popular among the experimental mechanics community, and both 2D-DIC and 3D-DIC are being increasingly used in a very wide range of applications

ranging from material science to manufacturing, mechanical, biomedical and structural engineering [5, 6].

The basic idea of DIC is to compare two digital images acquired at different states (e. g., one before deformation and the other one after), of a surface having a random speckle pattern, by dividing the image into subsets of several pixels then mathematically matching those subsets between the two images (based on intensity levels) to determine the new location of each subset in the second image. From that, the full-field deformation map can be obtained and the strain map can then be easily determined. In principle, 2D-DIC can be used for deformation measurements under three conditions; the specimen has a plannar surface, it undergoes in-plane deformations and the camera's optical axis is perpendicular to the specimen surface. If any of these three conditions is not reasonably satisfied, the accuracy of the measurements will be compromised. In one of the key papers addressing the applications of DIC in experimental mechanics, Chu et al. [7] used in-plane rigid-body-translations to demonstrate the viability of the DIC method for actual measurements. When a body undergoes a rigid-body-translation, the measured strains should theoretically be zero and thus any obtained strain readings reflect the magnitude of error in

\*Corresponding author: [hijazi@hu.edu.jo](mailto:hijazi@hu.edu.jo)

the measurement. This simple experiment remains to be one of the most widely used experiments for estimating the magnitude of background strain error expected in DIC strain measurements. The measurement accuracy of 2D-DIC depends on several factors which include; a) the speckle pattern, b) quality and perfection of the imaging system (distortions, noise, resolution, etc.) and c) the selection of the correlation algorithm and parameters (subset and step size, correlation and shape functions, sub-pixel algorithm, etc.) [3, 5]. Numerous studies have investigated the different sources of errors and tried to estimate the resulting errors and to suggest remedies in some cases. Listings of the different studies can be found in references [3, 5, 8, 9].

As mentioned earlier, the in-plane deformations and the perpendicularity of the viewing axis (i.e., the parallelism of the camera focal-plane-array with the specimen surface) are two of the basic assumptions for 2D-DIC. The occurrence of any out-of-plane translation or misalignment between the camera focal-plane-array and the specimen surface will lead to errors that are embedded in the measured displacements and strains. Out-of-plane translations may occur during the loading of the specimen, while the non-perpendicularity of the camera, on the other hand, may occur during loading (due to out-of-plane rotation of the specimen) or may exist before loading. Some recent studies [9-12] have investigated the errors caused by out-of-plane translations and/or non-perpendicular camera alignment. Haddadi et al. [9] did an experimental investigation where they used rigid-body-translations to investigate the different sources of error in 2D-DIC measurements and to estimate these errors. In that study, they estimated the strain errors induced by out-of-plane translations where they noted that; a) the error is linearly proportional to the amount out-of-plane displacement and b) for a fixed amount of out-of-plane displacement, the error decreases as the stand-off-distance between the camera and surface increases. Sutton et al. [10] studied the effects of out-of-plane displacements and rotations (that may occur during the loading) both theoretically and experimentally. Their results show that the strain error is proportional to the ratio  $\Delta Z/Z$  (where  $\Delta Z$  is the out-of-plane translation and  $Z$  is the stand-off-distance). They also showed that the use of telecentric lenses minimizes the error to a manageable level. Meng et al. [11] theoretically investigated the displacement errors caused by the camera non-perpendicularity and reported that the errors are linearly related to the displacement and non-perpendicularity when these two are small. Based on numerical analysis, they reported that measuring sensitivity of 0.01 pixels can be attained under misalignment angles up to 5 degrees. Lava et al. [12] studied the strain error caused by non-perpendicular camera alignment using numerically rotated images having an imposed finite element displacement field. They compared the strain error for a sample subjected to large plastic strain using 2D-DIC and 3D-DIC and proposed a method for rectifying the distorted image, resulting from camera non-perpendicularity, for 2D-DIC measurements. The proposed image rectification method helps in eliminating the error resulting from camera non-perpendicularity (e.g., when physical constraints prevent the camera from being oriented perpendicular to the surface) if the misalignment angle is known.

In this paper, we investigate the errors introduced in the measured strains resulting from camera non-

perpendicularity in 2D-DIC measurements both theoretically and experimentally. We also demonstrate the effect of the misalignment angle, in-plane translation and camera stand-off-distance on strain error. We show that simple in-plane rigid-body-translation experiments can be used to estimate the resulting strain errors and more importantly to detect, and hence correct, any existing non-perpendicularity between the camera's optical axis and the target surface. The development of the theoretical equations for estimating the strain errors (due to camera non-perpendicularity) associated with in-plane rigid-body-translations is presented in section 2. Section 3 presents the details of the experimental setup and the procedure used for measuring the DIC strain error at different camera orientation angles. The results of the theoretical and experimental investigation are presented in section 4 and the results are discussed in section 5. Finally, section 6 presents the concluding remarks.

## 2. Effect of Camera Non-perpendicularity on Strain Measurements

The perpendicularity of the camera's optical axis to the specimen surface is one of the three conditions, mentioned previously, for the validity of 2D-DIC measurements. When the camera is non-perpendicular to the specimen surface, in-plane translations of the specimen surface will not be faithfully replicated at the image plane. Consequently, DIC will show that the surface was deformed (strains not equal to zero) even if the surface underwent a pure rigid-body-translation. The resulting strain errors depend on the direction of in-plane translation relative to the camera tilt axis. If the translation is in the direction perpendicular to the tilt axis, it will change the actual stand-off-distance between the camera and all points on that surface and that in turn will change the magnification in both the x and y directions. Thus, DIC will show non-zero normal strain readings in both the x and y directions. On the other hand, if the translation is in the direction parallel to the tilt axis, points at different distances from the tilt axis will show different amounts of translation since they have different stand-off-distance from the camera. Therefore, DIC will show non-zero shear strain. In order to estimate the amount of strain error expected in DIC measurements, simple pinhole camera model can be used. According to pinhole imaging formulation, the imaged length,  $l^i$ , of an object of length  $l$  that is parallel to the image plane can be found as:

$$l^i = \frac{l}{D} f \quad (1)$$

where  $D$  is the distance between the camera and the object (i.e., the stand-off-distance) and  $f$  is the distance between the pinhole plane and the image plane (i.e., the focal distance). In geometric optics,  $f$  usually refers to the focal length of the lens which is slightly smaller than the distance to the image plane. However, it is reasonable to assume that  $f$  used in the pinhole camera formulation represents the focal length of a real lens.

Though DIC software packages calculate the strains based on the large strains theory (Green-Lagrange strain), for simplicity, small strains theory is used here for deriving the theoretical strain expressions. The obtained strain expressions are numerically evaluated using parameters matching those of the experimental setup. Since the expected strains are fairly small, the theoretically obtained

strain error values are expected to be in good agreement with the experimental values obtained using DIC software.

2.1. In-plane Translation Perpendicular to the Tilt Axis

Figure 1 shows a schematic for a pinhole camera imaging a surface where the surface is tilted about the  $y$  axis by an angle  $\theta$ . The surface rigidly translates along the  $x$  direction by a distance  $\Delta x$  and for clarity the positions of the surface before and after the translation are shown in two separate sketches as seen in the figure. To determine the amount of the induced “apparent” strain (i.e., strain error) when the surface rigidly moves from position (1) to position (2), two points on the surface (**A** and **B**) are considered. When the surface is at position (1), the  $x$  coordinates “at the image plane” for points **A** and **B** are found as:

$$(x_A^i)_1 = \frac{x_A \cos \theta}{S + x_A \sin \theta} f \tag{2}$$

$$(x_B^i)_1 = \frac{x_B \cos \theta}{S + x_B \sin \theta} f \tag{3}$$

where  $S$  is the nominal stand-off-distance between the camera and the surface and  $x_A$  &  $x_B$  are the coordinates of the two points “at position (1)”. The length of line **AB** at the image plane is simply found as:

$$(l_{AB}^i)_1 = (x_A^i)_1 - (x_B^i)_1 \tag{4}$$

When the surface rigidly translates a distance  $\Delta x$  to position (2), the  $x$  coordinates of the two points at the image plane become:

$$(x_A^i)_2 = \frac{(x_A - \Delta x) \cos \theta}{S + (x_A - \Delta x) \sin \theta} f \tag{5}$$

$$(x_B^i)_2 = \frac{(x_B - \Delta x) \cos \theta}{S + (x_B - \Delta x) \sin \theta} f \tag{6}$$

and the length of line **AB** at the image plane becomes:

$$(l_{AB}^i)_2 = (x_A^i)_2 - (x_B^i)_2 \tag{7}$$

Based on small strains theory, the average Cauchy strain in the  $x$  direction can be found as:

$$\epsilon_{xx} = \frac{(l_{AB}^i)_2 - (l_{AB}^i)_1}{(l_{AB}^i)_1} \tag{8}$$

Similarly, an “apparent” strain is also expected in the  $y$  direction. To determine the strain in the  $y$  direction, a line (oriented along the  $y$  direction) of length  $l_y$  that is located at an arbitrary distance  $x$  is considered. When the surface is at position (1), the length of that line “at the image plane” can be found as:

$$(l_y^i)_1 = \frac{l_y}{S + x \sin \theta} f \tag{9}$$

When the surface rigidly translates a distance  $\Delta x$  to position (2), the length of that line at the image plane becomes:

$$(l_y^i)_2 = \frac{l_y}{S + (x - \Delta x) \sin \theta} f \tag{10}$$

and the strain in the  $y$  direction can simply be found as:

$$\epsilon_{yy} = \frac{(l_y^i)_2 - (l_y^i)_1}{(l_y^i)_1} \tag{11}$$

2.2. In-plane Translation Parallel to the Tilt Axis

Figure 2 shows a schematic for a pinhole camera imaging a surface where the surface is tilted about the  $y$  axis by an angle  $\theta$  (similar to what is shown in figure 1 but the view is rotated 90° about the camera axis). The surface rigidly translates along the  $y$  direction by a distance  $\Delta y$  and two points on the surface (**A** and **B**) are considered. For simplicity, points **A** and **B** are defined along the  $x$  axis at arbitrary distance from the origin. The positions of points **A** and **B** before and after the translation are shown in the figure. Before the translation, the  $y$  coordinates of the two points are equal to zero. After the surface is rigidly translated by distance  $\Delta y$ , the  $y$  coordinates “at the image plane” for points **A** and **B** become:

$$y_A^i = \frac{\Delta y}{S + x_A \sin \theta} f \tag{12}$$

$$y_B^i = \frac{\Delta y}{S + x_B \sin \theta} f \tag{13}$$

Therefore, the shear strain can simply be found as:

$$\epsilon_{xy} = \frac{1}{2} \left( \frac{y_A^i - y_B^i}{x_A^i - x_B^i} \right) \tag{14}$$

where  $x_A^i$  and  $x_B^i$  (i.e., the  $x$  coordinates at the image plane for points **A** and **B**) are found using equations 2 and 3 given previously.

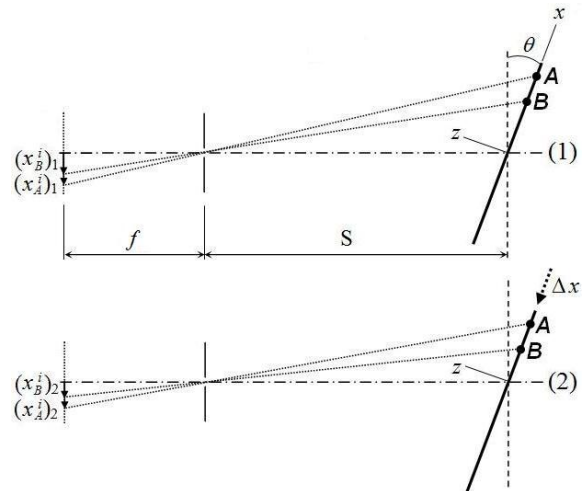


Figure 1. Non-perpendicular pinhole camera schematic; surface translating perpendicular to tilt axis.

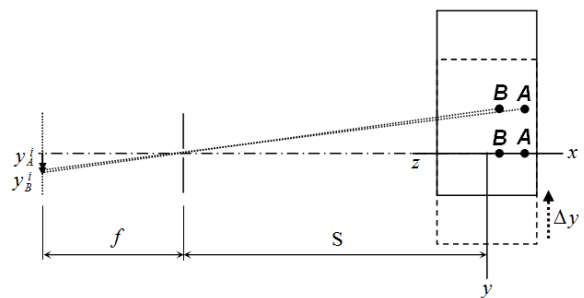


Figure 2. Non-perpendicular pinhole camera schematic (view rotated 90° about the camera axis); surface translating parallel to tilt axis.

### 3. Experiments

In order to experimentally quantify the DIC strain error resulting from camera non-perpendicularity, different groups of experiments were conducted where in the first group the camera was perfectly perpendicular to the surface and in each of the other groups the camera was tilted with a different angle (from 1° to 5° in 1° steps). A schematic view of the experimental setup is shown in figure 3. As can be seen from the figure, the camera was tilted around its own axis which is parallel to the  $y$  axis. In each group of experiments, while the camera is at a fixed angle with respect to the surface, the surface was translated in two steps along the  $x$  direction (i.e., perpendicular to the tilt axis) then in two steps along the  $y$  direction (i.e., parallel to the tilt axis). As a result, images were captured while the surface is at five different positions; a reference position, two translation steps in the  $x$  direction and two translation steps in the  $y$  direction.

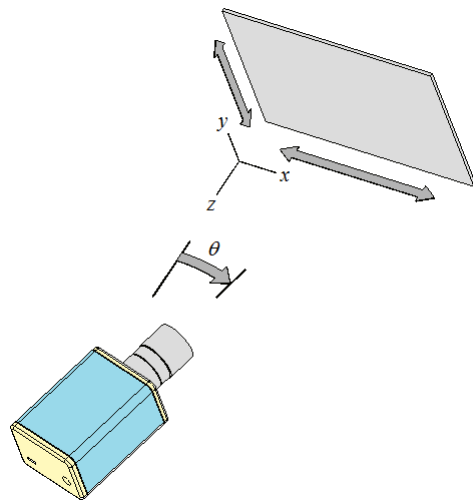


Figure 3. Schematic view for the setup used in the experiments.

The vision system used in this study consists of; a) DALSA Genie-M1410 camera having a 2/3 inch monochrome interline CCD chip with 1360×1024 pixel resolution, b) Pentax C5028-M machine vision lens having 50mm focal length, c) a 2mm extension ring between the lens and the camera to reduce the minimum working distance of the lens. The aperture of the lens was set to  $f/8$  to obtain a reasonable depth of field in order to accommodate the depth gradient resulting from camera non-perpendicularity. The camera was mounted on a rotating-stage to allow orienting the camera at the desired tilt angles. A printed black and white random speckle pattern was attached to the target surface which is mounted on a multi-axis translating stage. The distance between the front end of the lens and the target surface was set to about 680mm and at that working distance the field-of-view observed by the camera was about a 113mm wide (12 pixels/mm scale factor). At the magnification level provided by the vision system, the average diameter for the black dots of the speckle pattern was about 6 pixels and the average dot center-to-center spacing was about 13 pixels. Each of the two translation steps, in both the  $x$  and  $y$  directions, was equal to 8mm (about 7% of the field-of-view width). In the first group of experiments (i.e., camera perpendicular to the surface), the camera was first placed

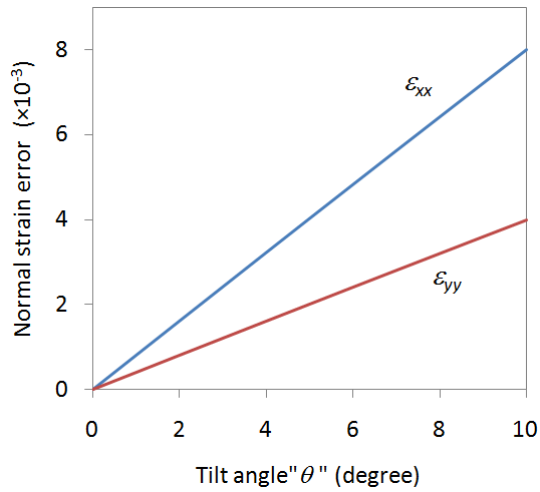
close to the surface and a right-angle triangle was used to verify its perpendicularity then it was translated backwards with the aid of an optical rail to the required working distance. In each of the preceding groups of experiments, the camera was tilted by 1° using the rotating stage and the same experiments were repeated.

For each group of experiments corresponding to a different camera orientation angle, the reference position image was correlated with the images corresponding each of the two translation steps in each of the two directions. Commercial 2D-DIC software called “VIC-2D” [13] was used for the analyses and the same analyses were also repeated (with identical parameters) using other software called “MatchID-2D” [14] for further verification of the results. A subset size of 41×41 pixels with a step size of 20 pixels was used for the correlation. The Green-Lagrange strains were calculated using a strain window size of 7×7 points. The entire area of the reference image was used for the correlation, rather than choosing a partial region of interest, such that a more reliable averages of the resulting strains can be obtained.

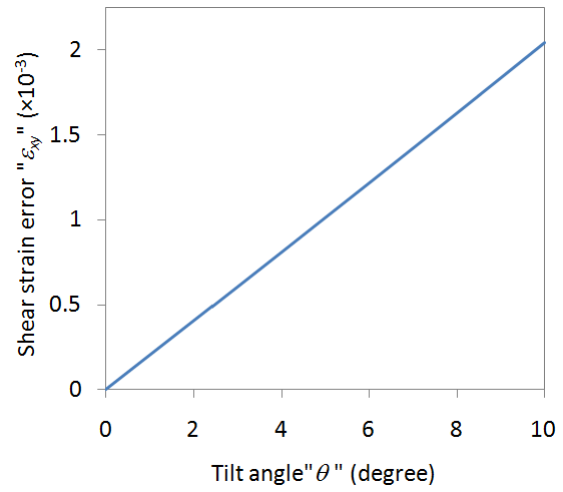
### 4. Results

#### 4.1. Theoretical Results

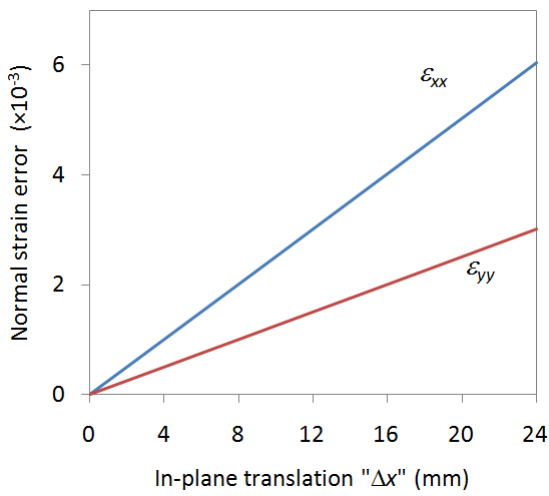
The normal strains ( $\epsilon_{xx}$  and  $\epsilon_{yy}$ ) error resulting from in-plane translation perpendicular to the tilt axis was obtained by solving equations 8 and 11 numerically using parameters similar to those of the experimental setup. It should be noted that some of the parameters involved in equations 8 and 11 has very minor or no effect on the obtained strain values. For instance, by substituting equations 2 through 7 into equation 8, the focal length  $f$  will cancel out from the equation and the same will happen in equation 11. Also, other parameters were found to have very insignificant influence on the results. However, values have to be assigned to these parameters for the numerical evaluation. The values of these parameters used in the evaluation are;  $x_A = 1$  mm,  $x_B = 0$  mm,  $l_y = 1$  mm and  $x = 1$  mm. On the contrary, the tilt angle  $\theta$ , the magnitude of in-plane-translation  $\Delta x$  and the stand-off-distance  $S$  have a significant influence on the resulting normal strains. The influence of these three parameters was investigated by considering an appropriate range for each and the results are shown in Figure 4. As can be seen from the figure, the strain error in the  $x$  direction (i.e., the direction of translation) is larger than that in the  $y$  direction where its value is twice of that in the  $y$  direction. From figure 4 (a) and (b) it can be seen that the strain error is linearly related to both the tilt angle and in-plane translation, while the strain error has an inverse relation with the stand-off-distance as seen in figure 4 (c). The inverse relation between stand-off-distance and the strain error is consistent with the findings reported previously in literature for the case of out-of-plane translation [9, 10]. This similarity is rather expected because, as mentioned earlier, in-plane translations occurring while the camera is non-perpendicular to the surface change the actual stand-off-distance between the camera and all points on that surface. It should be mentioned that in the theoretical analyses, the stand-off-distance  $S$  was set to be 690mm which is 10mm more than the actual distance between the front end of the lens and the target surface. The reason for adding this 10mm was to account for the distance from the front end of the lens to its optical center.



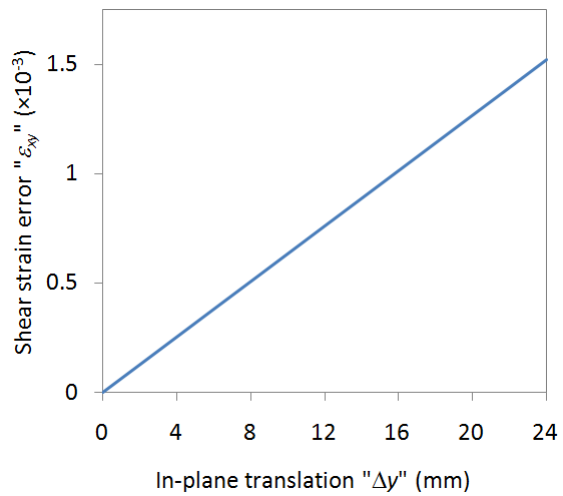
(a)



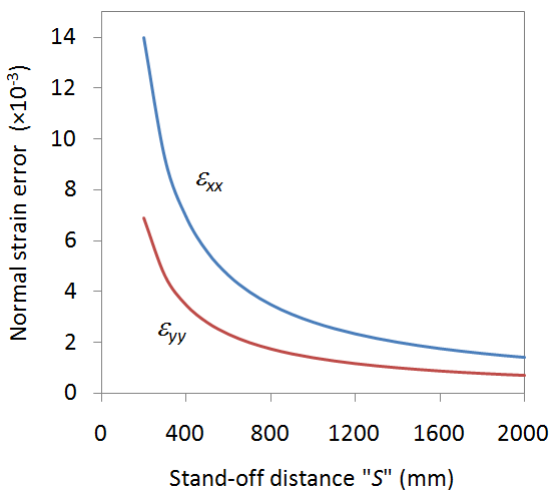
(a)



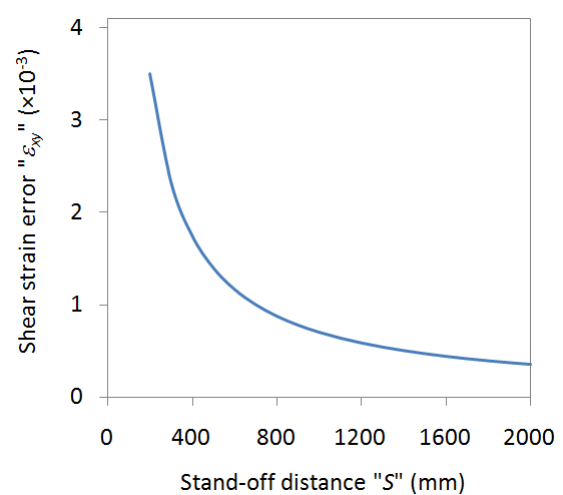
(b)



(b)



(c)



(c)

Figure 4. Normal strain error resulting from rigid-body in-plane translation in the direction perpendicular to the tilt axis; **a)** influence of tilt angle ( $S = 690$  mm &  $\Delta x = 16$  mm), **b)** influence of the magnitude of translation ( $S = 690$  mm &  $\theta = 5^\circ$ ), **c)** influence of stand-off-distance ( $\Delta x = 16$  mm &  $\theta = 5^\circ$ ).

Figure 5. Shear strain error resulting from rigid-body in-plane translation in the direction parallel to the tilt axis; **a)** influence of tilt angle ( $S = 690$  mm &  $\Delta y = 16$  mm), **b)** influence of the magnitude of translation ( $S = 690$  mm &  $\theta = 5^\circ$ ), **c)** influence of stand-off-distance ( $\Delta y = 16$  mm &  $\theta = 5^\circ$ ).

Similarly, the shear strain error resulting from in-plane translation parallel to the tilt axis was obtained by solving equation 14 numerically using parameters similar to those of the experimental setup. Again, by substituting in the equation, the focal length  $f$  cancels out and the assigned values for the other parameters are;  $x_A = 1$  mm and  $x_B = 0$  mm. The influence of the tilt angle  $\theta$ , the magnitude of in-plane-translation  $\Delta y$  and the stand-off-distance  $S$  on shear strain error are shown in figure 5. From the figure it can be seen that the influence of these three parameters on the shear strain error is similar to that on the normal strains error seen previously in figure 4. By closely inspecting the values of shear strain error, it can be seen that its magnitude is one fourth of that of the normal strain  $\epsilon_{xx}$  error resulting from in-plane translation perpendicular to the tilt axis.

It should be mentioned here that though the focal length  $f$  cancels out from the equations used for calculating the strain (eqns. 8, 11 and 14), the strain error depends of the focal length of the lens being used. This is simply due to the fact that in any experiment, certain magnification factor is required according to the size of specimen being observed. Therefore, to increase the stand-off-distance while maintaining the magnification, a higher focal length lens needs to be used. Practically, this means that the focal length have the same influence on strain error as the stand-off-distance.

#### 4.2. DIC Results

As mentioned previously, at each value of the tilt angle four correlations were carried out. In each correlation, the same reference image was correlated with one of the four translated images corresponding to in-plane translations in the  $x$  or  $y$  directions with a translation value of 8mm or 16 mm. Figure 6 shows an exemplary DIC output for 16mm translation in the  $x$  direction (i.e., the direction perpendicular to the tilt axis) where the camera was tilted by 5 degrees. From 6 (a) it can be seen that the results shows a clear gradient along the  $x$  direction of more than four pixels in the value of the horizontal translation ( $U$ ) though the surface was rigidly translated. A similar gradient but of smaller magnitude and different direction is also observed in the vertical translation ( $V$ ) values, as can be seen in 6 (b), though the surface was not translated in the vertical direction. It can be seen from the figure that these gradients are slightly rotated where that is most likely due to a very small amount of in-plane rotation that happened during the translation. These gradients in the translation values give indication to the magnitude of the error in measured displacements resulting from camera non-perpendicularity where, for instance, the four pixels difference in the horizontal displacement value simply represents the magnitude of displacement error (over the entire field-of-view) in the measurement. The presence of such gradients in the translation values indicates that the

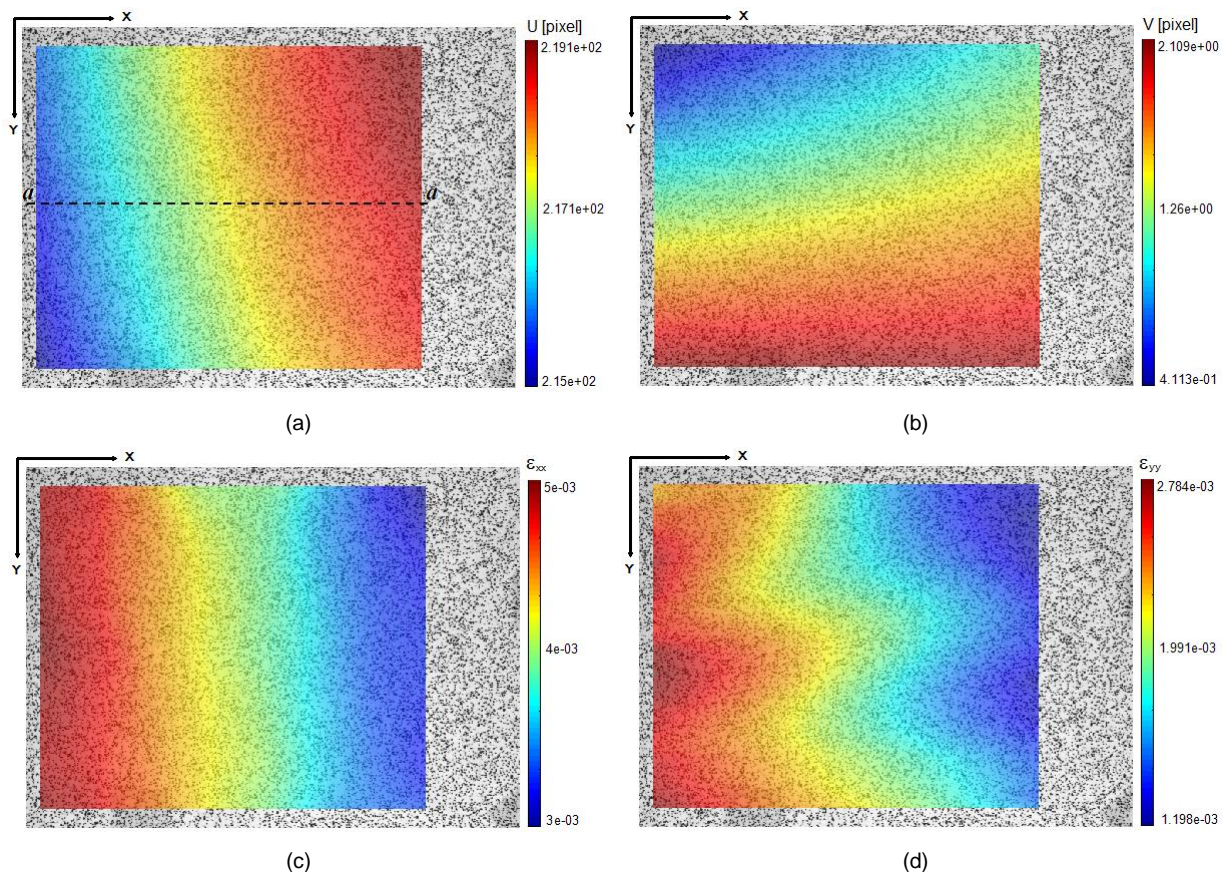


Figure 6. Typical DIC results for in-plane rigid-body-translation in the direction perpendicular to the tilt axis ( $\theta = 5^\circ$ ,  $\Delta x = 16$  mm); **a**) measured horizontal displacement, **b**) measured vertical displacement, **c**) measured normal strain in  $x$  direction, **d**) measured normal strain in  $y$  direction.

strains in both directions have non-zero values (the values of these strains represent the strain error in the measurement). The resulting normal strain errors in the  $x$  and  $y$  directions can be seen in 6 (c) and (d). From the figure it can be seen that the strain in the  $x$  direction is larger than that in the  $y$  direction where that is consistent with the theoretical results presented earlier which shows that  $\epsilon_{xx}$  is twice of  $\epsilon_{yy}$ . The figure also shows a large gradient along the  $x$  direction in the values of both  $\epsilon_{xx}$  and  $\epsilon_{yy}$ . This gradient in the strain value,  $\epsilon_{xx}$  for instance, indicates that the horizontal translation ( $U$ ) is not linearly related to the  $x$  position as will be discussed in the next section.

Similarly, figure 7 shows DIC results for 16mm translation in the  $y$  direction (i.e., the direction parallel to the tilt axis) with 5 degrees camera tilt angle. From 7 (a) it can be seen that the horizontal translation ( $U$ ) is fairly uniform (the slight non uniformity seen in the figure is most likely due to the lens optical distortions) and has a very small value. However, on the contrary, the vertical displacement ( $V$ ) shows a clear gradient along the  $x$  direction, as can be seen in 7 (b), which indicates a non-zero shear strain. The resulting shear strain error is shown in 7 (c) where it can be seen that it has a large gradient along the  $x$  direction as well.

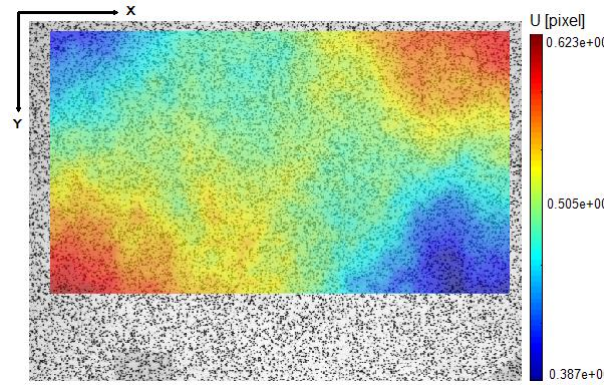
**5. Discussion**

The experimental results presented in the previous section confirms the theoretical conclusion that in-plane translations perpendicular to the tilt axis cause normal strain error while translations parallel to the tilt axis cause shear strain error. However, as mentioned earlier, equations 8, 11 and 14 which are used for calculating the strain error values are dependent on three parameters only (the tilt angle, the magnitude of in-plane-translation and the stand-off-distance). This indicates that the strain error values calculated by these equations are uniform over the entire surface. While, on the other hand, the DIC results show an obvious gradient in the strain values along the  $x$  direction. In order to understand the reason behind this difference, the horizontal translation at the image plane when the surface translates a distance  $\Delta x$  along the  $x$  direction is calculated as:

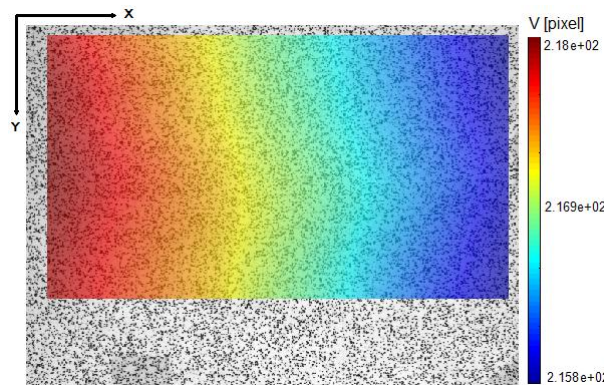
$$U^i = (x^i)_2 - (x^i)_1 \tag{15}$$

where  $(x^i)_1$  and  $(x^i)_2$  are the  $x$  coordinates “at the image plane” of a point on the surface before and after the surface is rigidly translated. The values of  $(x^i)_1$  and  $(x^i)_2$  can be calculated using equations 2 and 5, respectively. By assigning an appropriate range of values for  $x_A$  and substituting the correct values for the other parameters, the horizontal displacement as a function of the  $x$  position “at the image plane” can be obtained. Figure 8 shows the experimental relation between the horizontal translation and the  $x$  position which is obtained along the horizontal line “ $a-a$ ” taken in the middle of the image as seen in figure 6 (a). Figure 8 also shows the theoretical relation obtained from equation 15, using the same parameters of that experiment, after being scaled to be plotted in “pixel” units. From the figure it can be seen that the theoretical analysis gives a linear relation while the DIC yields a nonlinear relation, while both relations still give the same net value change of about four pixels over the entire field-of-view width. This difference between the theoretical and experimental relations indicates that the simple pinhole

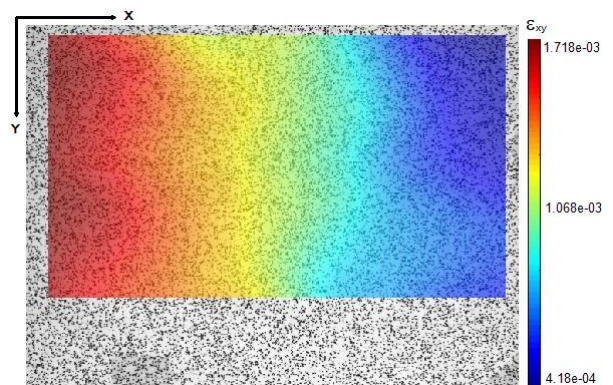
camera model used in developing the theoretical equations does not accurately replicate the behavior of real lenses when depth gradients are involved. It can also be seen from the figure that the theoretical normal strain  $\epsilon_{xx}$  will have a constant value that equals the derivative of the  $U$  with respect to  $x$  which is simply the slope of the straight line. On the other hand, when the derivative of the experimental curve is taken, that will give a normal strain  $\epsilon_{xx}$  value that varies along the  $x$  direction as seen previously in figure 6 (c).



(a)



(b)



(c)

Figure 7. Typical DIC results for in-plane rigid-body-translation in the direction parallel to the tilt axis ( $\theta = 5^\circ$ ,  $\Delta y = 16$  mm) : **a**) measured horizontal displacement, **b**) measured vertical displacement, **c**) measured shear strain.

In order to compare the experimentally measured strain error values with the theoretical estimates, the “mean” strain value ( $\frac{1}{N} \sum \epsilon$ ) for each strain component ( $\epsilon_{xx}$ ,  $\epsilon_{yy}$  and

$\epsilon_{xy}$ ) was calculated over the entire area of the image for each experiment. Figure 9 shows a comparison of the experimental and theoretical normal strain error values resulting from in-plane translation in the direction perpendicular to the tilt axis. Figure 10 shows the same comparison for shear strain error resulting from in-plane translation in the direction parallel to the tilt axis. From both figures it can be seen that the experimental results are in very good agreement with the theoretical estimates. The figures also show that the biggest difference between the experimental results and the theoretical values is observed when the camera is perfectly perpendicular to the surface where the theoretical analyses predict that all strain components are equal to zero while the experiments show small magnitudes of strain error. The experimental error observed there is mainly due to the optical distortions caused by the imaging system. The results show that, for the experimental setup used here, an in-plane translation of 16mm (i.e., about 14% of the field-of-view width) can cause a normal strain error as high as  $4 \times 10^{-3}$  at  $5^\circ$  tilt angle and the error will be even higher for shorter camera stand-off-distance. While such value of strain error might not seem that noteworthy if large plastic strains are being measured, but in fact such error value is significant knowing that it exceeds the elastic strain limit for many metallic alloys. It should also be noted that the magnitude of the strain error is not uniform over the entire surface area (see figures 6 and 7) and more variation in the error values will be present when making measurements of a surface undergoing deformation. These results clearly show that in-plane rigid-body-translations of the surface being measured using 2D-DIC can be used for detecting any misalignment between the surface and the camera focal plane array. The magnitude of the misalignment angle, if present, can be calculated using simple theoretical equations such as those presented in this paper. The calculation of the misalignment angle can be useful in cases where physical constrains prevent the camera from being oriented perpendicular to the surface. In such case the images can be rectified using an approach similar to that proposed by Lava et al. [12].

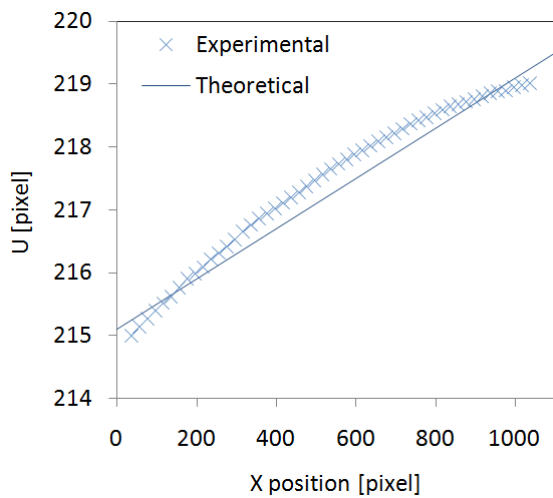
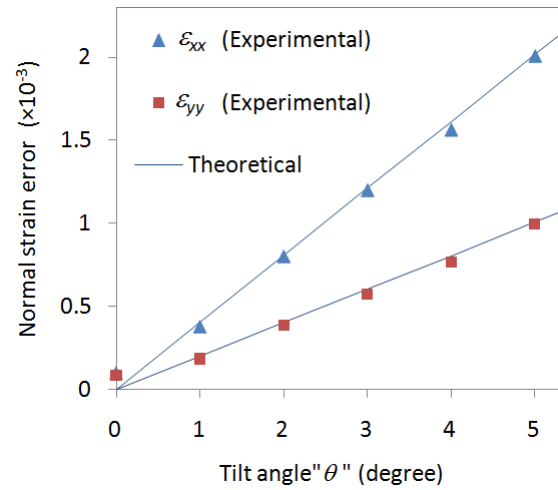
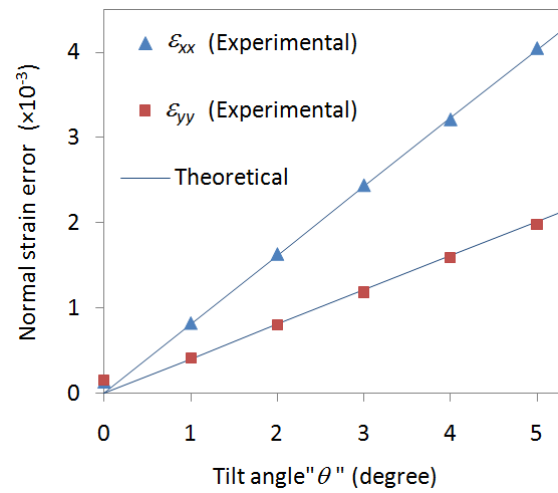


Figure 8. Comparison of the theoretically predicted and experimentally obtained relation between the horizontal translation and the position along the image x axis ( $\theta = 5^\circ$ ,  $\Delta x = 16$  mm).



(a)



(b)

Figure 9. Comparison of experimentally measured “mean” normal strains error with theoretical values for in-plane translation in the direction perpendicular to the tilt axis; a)  $\Delta x = 8$  mm, b)  $\Delta x = 16$  mm.

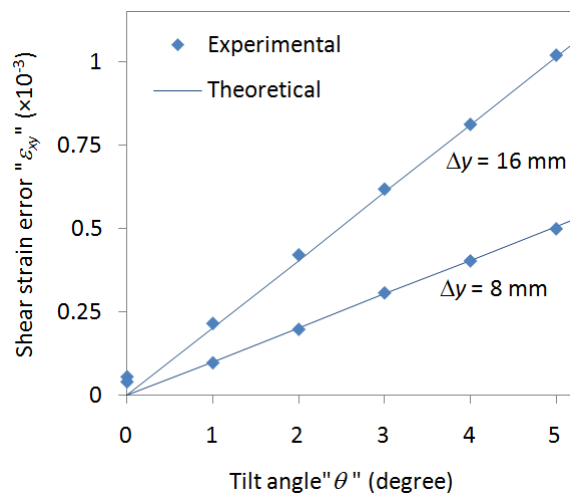


Figure 10. Comparison of experimentally measured “mean” shear strain error with theoretical values for in-plane translation in the direction parallel to the tilt axis.

In most realistic scenarios, the initial adjustment of the camera orientation with respect to the target surface is done manually without the use of any tools for angle measurement. In such cases, misalignment angles of up to two or three degrees are very well likely to go unnoticed and it is usually assumed that the DIC measurement error resulting from such small angular misalignments is negligible. The results presented here show that a misalignment angle as small as  $2^\circ$  can result in a strain error of more than  $10^3 \mu$ -strains for an in-plane displacement of 14% of the field-of-view width. Such magnitude of error is enormous when the expected strains are not large, such as the measurement of elastic properties of materials. Though it is possible to measure the exact value of the misalignment angle using the simple equations presented here, in most cases, it is not very practical to do so. In principle, it is possible to use in-plane rigid-body-translations to identify the presence of any misalignment simply by inspecting the magnitudes of strain errors resulting from these translations. However, the fact that the magnitude of strain error depends on several factors (e.g., the optical system, the speckle pattern, the correlation parameters, etc.) makes it difficult to make such judgment. Figure 11 (a) shows the distribution of normal strain error (a histogram but shown using lines for ease of view) resulting from 16mm translation in the  $x$  direction at three different values of camera tilt angle. At zero degrees (i.e., camera is perpendicular), the error is completely random and its mean value is very close to zero. As mentioned earlier, the error in this case is mostly due to optical distortions caused by the imaging system. As the camera tilt angle increases, the error distribution is shifted (to the positive or negative direction according to the direction of tilt angle and direction of in-plane translation) due to the additional error caused by the camera non-perpendicularity. By calculating the “mean” value of the error ( $\frac{1}{N} \sum \epsilon$ ) and the “mean of the absolute values” ( $\frac{1}{N} \sum |\epsilon|$ ) and showing them versus the tilt angle, figure 11 (b), an interesting observation can be made. As can be seen from the figure, when the camera is perpendicular, there is a big difference between the magnitudes of the mean and the mean of absolute values of strain error. As the tilt angle increases, the mean starts approaching the mean of absolute values and at  $1^\circ$  their magnitudes become almost identical (for angles larger than one degree, they will have the exact same magnitude). This clearly indicates that it is possible to detect camera non-perpendicularity simply by calculating the “mean” and the “mean of absolute values” of strain errors and comparing their magnitudes. If their magnitudes are identical, or very close to each other, this means that the camera is tilted, and thus attempts can be made to correct its orientation. From figure 11 (b) it can be seen that for the experimental setup used here, misalignment angles smaller than  $1^\circ$  can be detected. Furthermore, the results presented in this paper indicate that a translation in one direction,  $x$  direction for instance, can indicate whether the camera is tilted around the  $x$  axis or the  $y$  axis (or both) since the normal strains error indicates that the camera is tilted around the  $y$  axis (i.e., the axis perpendicular to the translation direction) and the shear strain error indicates that it is tilted around the  $x$  axis (i.e., the axis parallel to the translation direction).

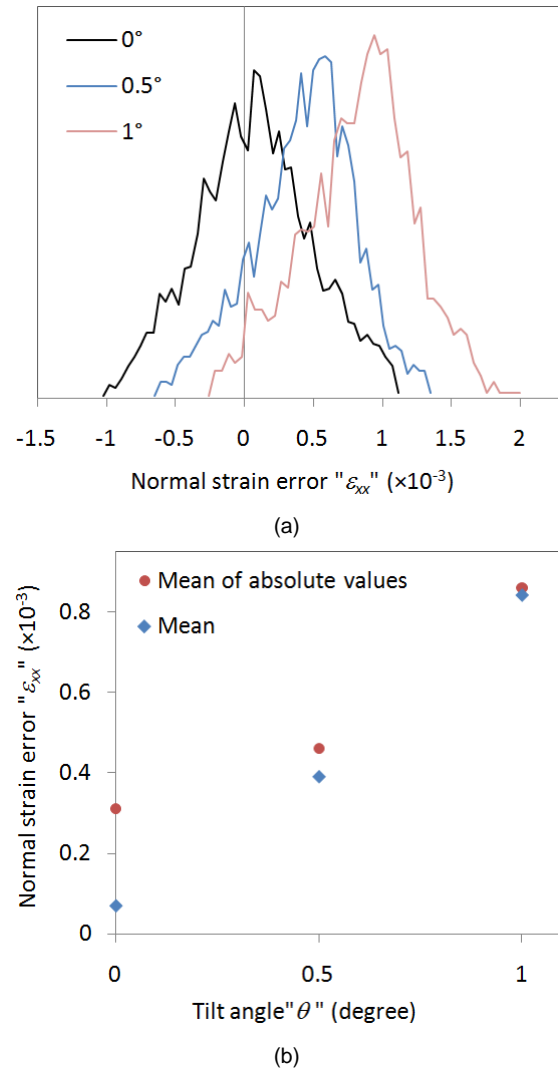


Figure 11. Experimentally measured normal strain error resulting from in-plane translation ( $\Delta x = 16$  mm) at different tilt angles; **a**) error distribution histogram, **b**) the “mean” and the “mean of absolute values” of error.

## 6. Concluding Remarks

In this work we investigated the influence of the camera’s optical axis non-perpendicularity to the surface being observed on strain measurements errors both theoretically and experimentally. Theoretical models were developed based on simple pinhole camera model to estimate the errors in the measured normal and shear strains associated with in-plane translations in the directions perpendicular and parallel to the camera tilt axis. The conclusions of this investigation can be summarized in the following points.

- When the camera’s optical axis is not perpendicular to the surface being observed, any in-plane translation in the direction perpendicular or parallel to the camera tilt axis will cause errors in strain measurements.
- In-plane translations in the direction perpendicular to the camera tilt axis cause errors in both normal strain components.
- In-plane translations in the direction parallel to the camera tilt axis cause error in shear strain.

- In-plane rigid-body-translations can be used for estimating the resulting normal and shear strain errors.
- Theoretical equations based on simple pinhole camera model cannot predict the actual gradient of the strain errors resulting from camera non-perpendicularity; however, they can predict the mean values of strain errors.
- The magnitude of error in all strain components increases linearly with the tilt angle (for the range of angles investigated here; up to 5°) and the magnitude of in-plane translation.
- The strain error is inversely related to the stand-off-distance and, practically, the same can be said about the focal length of the lens when a constant magnification factor is desired.
- Misalignment angles as small as 2°, which could be easily overlooked during the initial setting of the experimental setup, are found to cause strain error greater than  $10^3 \mu$ -strains.
- The theoretical strain error analyses are in very good agreement with the mean values of the strain errors measured experimentally. This indicates that the simple theoretical models presented here can be used to estimate the camera tilt angle and hence correct any existing non-perpendicularity between the camera's optical axis and the target surface.
- Simple in-plane rigid-body-translation experiments can be used to detect any existing non-perpendicularity between the camera's optical axis and the target surface by comparing the magnitudes of the "mean" and the "mean of absolute values" of strain errors. Experiments show that misalignment angles smaller than 1° can be detected.
- An in-plane translation in one direction ( $x$  or  $y$ ) can indicate whether the camera is tilted around the  $x$  axis or the  $y$  axis (or both) since the normal strains errors are associated with translations perpendicular to the tilt axis and the shear strain error is associated with translations parallel to the tilt axis.

### Acknowledgment

The first author is pleased to acknowledge the financial support provided by the German Research Foundation (DFG) for funding his research visit to the Institute of Fluid Mechanics and Aerodynamics at Universität der Bundeswehr München. He also acknowledges the support provided by the Deanship of Scientific Research at the Hashemite University for covering his travel expenses.

### References

- [1] Sutton, M., Wolters, W., Peters, W., Ranson, W. and McNeill, S., "Determination of displacement using an improved digital correlation method", *Image and Vision Computing*, Vol. 1, 1983, 133-139
- [2] Sutton, M., McNeill, S., Helm, J. and Chao, Y., "Advances in two-dimensional and three-dimensional computer vision", *Topics in Applied Physics*, Vol. 77, ed. Rastogi P (Berlin: Springer), 2000, p. 323-372
- [3] Sutton, M., Orteu, J. and Schreier, H., *Image Correlation for Shape, Motion and Deformation Measurements*, New York: Springer, 2009
- [4] Luo, P., Chao, Y., Sutton, M. and Peters, W., "Accurate measurement of three-dimensional deformations in deformable and rigid bodies using computer vision", *Experimental Mechanics*, Vol. 33, 1993, 123-132
- [5] Pan, B., Qian, K., Xie, H. and Asundi, A., "Two-dimensional digital image correlation for in-plane displacement and strain measurement: a review", *Measurement Science and Technology*, Vol. 20, 062001, 2009, (17pp)
- [6] Orteu, J., "3-D computer vision in experimental mechanics", *Optics and Lasers in Engineering*, Vol. 47, 2009, 282-291
- [7] Chu, T., Ranson, W., Sutton, M. and Peters, W., "Applications of digital-image-correlation techniques to experimental mechanics", *Experimental Mechanics*, Vol. 25, 1984, 232-244
- [8] Bornert, M., Brémand, F., Doumalin, P., Dupré, J., Fazzini, M., Grédiac, M., Hild, F., Mistou, S., Molimard, J., Orteu, J., Robert, L., Surrel, Y., Vacher, P. and Wattrisse, B., "Assessment of digital image correlation measurement errors: methodology and results", *Experimental Mechanics*, Vol. 49, 2009, 353-370
- [9] Haddadi, H. and Belhabib, S., "Use of rigid-body motion for the investigation and estimation of the measurement errors related to digital image correlation technique", *Optics and Lasers in Engineering*, Vol. 46, 2008, 185-196
- [10] Sutton, M., Yan, J., Tiwari, V., Schreier, H. and Orteu, J., "The effect of out-of-plane motion on 2D and 3D digital image correlation measurements", *Optics and Lasers in Engineering*, Vol. 46, 2008, 746-757
- [11] Meng, L., Jin, G. and Yao, X., "Errors caused by misalignment of the optical camera axis and the object surface in the DSCM", *Journal of Tsinghua University (Science and Technology)*, Vol. 46, 2006, 1930-1932
- [12] Lava, P., Coppieters, S., Wang, Y., Van-Houtte, P. and Debruyne, D., "Error estimation in measuring strain fields with DIC on planar sheet metal specimens with a non-perpendicular camera alignment", *Optics and Lasers in Engineering*, Vol. 49, 2011, 57-65
- [13] VIC-2D manual, < [www.CorrelatedSolutions.com](http://www.CorrelatedSolutions.com) >
- [14] MatchID-2D manual, < [www.MatchID.org](http://www.MatchID.org) >